Improved Measurement of $|V_{cb}|$ Using $\overline{B} \to D^* \ell \overline{\nu}$ Decays

R. A. Briere,[1] G. P. Chen,[1] T. Ferguson,[1] G. Tatishvili,[1] H. Vogel,[1] N. E. Adam,[2] J. P. Alexander,[2] C. Bebek,[2] B. E. Berger,[2] K. Berkelman,[2] F. Blanc,[2] V. Boisvert,[2] D. G. Cassel,[2] P. S. Drell,[2] J. E. Duboscq,[2] K. M. Ecklund,[2] R. Ehrlich,[2] L. Gibbons,[2] B. Gittelman,[2] S. W. Gray,[2] D. L. Hartill,[2] B. K. Heltsley,[2] L. Hsu,[2] C. D. Jones,[2] J. Kandaswamy,[2] D. L. Kreinick,[2] A. Magerkurth,[2] H. Mahlke-Krüger,[2] T. O. Meyer,[2] N. B. Mistry,[2] E. Nordberg,[2] M. Palmer,[2] J. R. Patterson,[2] D. Peterson,[2] J. Pivarski,[2] D. Riley,[2] A. J. Sadoff,[2] H. Schwarthoff,[2] M. R. Shepherd,[2] J. G. Thayer,[2] D. Urner,[2] B. Valant-Spaight,[2] G. Viehhauser,[2] A. Warburton,[2] M. Weinberger,[2] S. B. Athar,[3] P. Avery,[3] H. Stoeck,[3] J. Yelton,[3] G. Brandenburg,[4] A. Ershov,[4] D. Y.-J. Kim,[4] R. Wilson,[4] K. Benslama,[5] B. I. Eisenstein,[5] J. Ernst,[5] G. D. Gollin,[5] R. M. Hans,[5] I. Karliner,[5] N. Lowrey,[5] M. A. Marsh,[5] C. Plager,[5] C. Sedlack,[5] M. Selen,[5] J. J. Thaler,[5] J. Williams,[5] K. W. Edwards,[6] R. Ammar,[7] D. Besson,[7] X. Zhao,[7] S. Anderson,[8] V. V. Frolov,[8] Y. Kubota,[8] S. J. Lee,[8] S. Z. Li,[8] R. Poling,[8] A. Smith,[8] C. J. Stepaniak,[8] J. Urheim,[8] S. Ahmed,[9] M. S. Alam,[9] L. Jian,[9] M. Saleem,[9] F. Wappler,[9] E. Eckhart,[10] K. K. Gan,[10] C. Gwon,[10] T. Hart,[10] K. Honscheid,[10] D. Hufnagel,[10] H. Kagan,[10] R. Kass,[10] T. K. Pedlar,[10] J. B. Thayer,[10] E. von Toerne,[10] T. Wilksen,[10] M. M. Zoeller,[10] S. J. Richichi,[11] H. Severini,[11] P. Skubic,[11] S. A. Dytman,[12] S. Nam,[12] V. Savinov,[12] S. Chen,[13] J. W. Hinson,[13] J. Lee,[13] D. H. Miller,[13] V. Pavlunin,[13] E. I. Shibata,[13] I. P. J. Shipsey,[13] D. Cronin-Hennessy,[14] A. L. Lyon,[14] C. S. Park,[14] W. Park,[14] E. H. Thorndike,[14] T. E. Coan,[15] Y. S. Gao,[15] F. Liu,[15] Y. Maravin,[15] I. Narsky,[15] R. Stroynowski,[15] J. Ye,[15] M. Artuso,[16] C. Boulahouache,[16] K. Bukin,[16] E. Dambasuren,[16] R. Mountain,[16] T. Skwarnicki,[16] S. Stone,[16] J. C. Wang,[16] A. H. Mahmood,[17] S. E. Csorna,[18] I. Danko,[18] Z. Xu,[18] G. Bonvicini,[19] D. Cinabro,[19] M. Dubrovin,[19] S. McGee,[19] A. Bornheim,[20] E. Lipeles,[20] S. P. Pappas,[20] A. Shapiro,[20] W. M. Sun,[20] A. J. Weinstein,[20] G. Masek,[21] H. P. Paar,[21] and R. Mahapatra[22]

(CLEO Collaboration)

[1]*Carnegie Mellon University, Pittsburgh, Pennsylvania 15213*
[2]*Cornell University, Ithaca, New York 14853*
[3]*University of Florida, Gainesville, Florida 32611*
[4]*Harvard University, Cambridge, Massachusetts 02138*
[5]*University of Illinois, Urbana-Champaign, Illinois 61801*
[6]*Carleton University, Ottawa, Ontario, Canada K1S 5B6 and the Institute of Particle Physics, Canada M5S 1A7*
[7]*University of Kansas, Lawrence, Kansas 66045*
[8]*University of Minnesota, Minneapolis, Minnesota 55455*
[9]*State University of New York at Albany, Albany, New York 12222*
[10]*The Ohio State University, Columbus, Ohio 43210*
[11]*University of Oklahoma, Norman, Oklahoma 73019*
[12]*University of Pittsburgh, Pittsburgh, Pennsylvania 15260*
[13]*Purdue University, West Lafayette, Indiana 47907*
[14]*University of Rochester, Rochester, New York 14627*
[15]*Southern Methodist University, Dallas, Texas 75275*
[16]*Syracuse University, Syracuse, New York 13244*
[17]*University of Texas–Pan American, Edinburg, Texas 78539*
[18]*Vanderbilt University, Nashville, Tennessee 37235*
[19]*Wayne State University, Detroit, Michigan 48202*
[20]*California Institute of Technology, Pasadena, California 91125*
[21]*University of California, San Diego, La Jolla, California 92093*
[22]*University of California, Santa Barbara, California 93106*

(Received 11 March 2002; published 6 August 2002)

We determine the weak coupling $|V_{cb}|$ between the b and c quarks using a sample of 3×10^6 $B\bar{B}$ events in the CLEO detector at the Cornell Electron Storage Ring. We determine the yield of reconstructed $\bar{B} \to D^* \ell \bar{\nu}$ decays as a function of w, the boost of the D^* in the B rest frame, and from this we obtain the differential decay rate $d\Gamma/dw$. By extrapolating $d\Gamma/dw$ to $w = 1$, the kinematic end point at which the D^* is at rest relative to the B, we extract the product $|V_{cb}|\mathcal{F}(1)$, where $\mathcal{F}(1)$ is the form factor at $w = 1$. Combined with theoretical results for $\mathcal{F}(1)$ we determine $|V_{cb}| = 0.0469 \pm 0.0014(\text{stat}) \pm 0.0020(\text{syst}) \pm 0.0018(\text{theor})$.

DOI: 10.1103/PhysRevLett.89.081803 PACS numbers: 12.15.Hh, 13.20.He

In the standard model, the weak decay of quarks is described by a unitary 3×3 matrix [1]. This Cabibbo-Kobayashi-Maskawa (CKM) matrix describes the flavor mixing among the quarks and the amount of CP violation through its single nontrivial phase. Precise determinations of the CKM matrix elements are essential to test the standard model. This Letter presents an improved measurement of $|V_{cb}|$, the coupling of the b quark to the c quark. The CKM matrix element $|V_{cb}|$ sets the length of the base of the unitarity triangle (UT) [2], which displays one CKM unitarity condition, and normalizes the constraint on the UT from indirect CP violation in K^0 decay [3].

One strategy for determining $|V_{cb}|$ uses the decays $\bar{B}^0 \to D^{*+}\ell\bar{\nu}$ and $B^- \to D^{*0}\ell\bar{\nu}$, where ℓ indicates e^- or μ^- [4]. The rate for these decays, however, depends not only on $|V_{cb}|$ and well-known weak decay physics, but also on strong interaction effects, parametrized by form factors. In general, these effects are difficult to quantify, but heavy quark effective theory (HQET) offers a method for calculating them at the kinematic point at which the final-state D^* is at rest with respect to the initial B meson [5]. In this analysis [6], we take advantage of this information: we divide the reconstructed candidates into bins of w, where w is the scalar product of the B and D^* four velocities and is equivalent to the Lorentz boost E_{D^*}/M_{D^*} of the D^* in the B rest frame. Using these yields, we measure the differential rate $d\Gamma/dw$ for $w > 1$, and extrapolate to obtain the rate at $w = 1$, which, combined with theoretical results, gives $|V_{cb}|$.

We analyze 3.33×10^6 $B\bar{B}$ events (3.1 fb^{-1}) produced on the $\Upsilon(4S)$ resonance at the Cornell Electron Storage Ring (CESR) and detected in the CLEO II detector [7]. In addition, we use 1.6 fb^{-1} of data collected slightly below the $\Upsilon(4S)$ resonance for the purpose of determining continuum $e^+e^- \to q\bar{q}$ ($q = u, d, s, c$) backgrounds.

To identify D^* candidates, we reconstruct the decay chains $D^{*+} \to D^0\pi^+$ and $D^{*0} \to D^0\pi^0$ followed by $D^0 \to K^-\pi^+$. We first combine kaon and pion candidates in hadronic events to form D^0 candidates. Signal candidates lie in the mass window $|m(K\pi) - 1865| \leq 20$ MeV/c^2. We then add a slow π to the D^0 candidate to form a D^*. For D^{*+} (D^{*0}) candidates we require $\Delta m \equiv m(K\pi\pi) - m(K\pi)$ to be within 2 MeV/c^2 (3 MeV/c^2) of the known $D^{*+} - D^0$ ($D^{*0} - D^0$) mass difference. For D^{*+} candidates, the K and π are fit to a common vertex, and then the slow π and D are fit to a second vertex using a beam spot constraint. These constraints improve the Δm resolution by about 20%.

To D^* candidates we add a lepton candidate. We select electrons using the ratio of the energy deposited in the CsI calorimeter to the reconstructed track momentum, the shape of the shower in the calorimeter, and the specific ionization in the drift chamber. Our candidates lie in the momentum range $0.8 < p_e \leq 2.4$ GeV/c. We require muon candidates to penetrate ≈ 5 interaction lengths, which restricts their momentum range to $1.4 < p_\mu \leq 2.4$ GeV/c. The charge of the lepton must match the charge of the kaon and, for D^{*+} candidates, be opposite that of the slow pion.

For each candidate we compute the cosine of the angle $\theta_{B-D^*\ell}$ between the $\bar{B}$ and the combined $D^*\ell$ momenta using energy-momentum conservation and the assumption that a massless neutrino recoils against the $D^*\ell$ pair:

$$\cos\theta_{B-D^*\ell} = \frac{2E(B)E(D^*\ell) - m_B^2 - m(D^*\ell)^2}{2|\mathbf{p}(B)||\mathbf{p}(D^*\ell)|}. \quad (1)$$

This quantity helps distinguish signal from background, such as $\bar{B} \to D^*\pi\ell\bar{\nu}$, where additional particles are in the final state, leading to nonphysical values. This angle also improves our determination of w, for which we need to know the B rest frame. Although the magnitude of the B momentum is known, the B direction is unknown. However, it must lie on a cone with opening angle $\theta_{B-D^*\ell}$ around the $D^*\ell$ direction. We calculate w for all B flight directions on this cone and average the smallest and largest values to estimate w, with a typical resolution of 0.03. We divide our sample into ten bins from 1.0 to 1.5, the final bin including candidates up to the kinematic limit of 1.504. For $w > 1.25$, we suppress background with no loss of signal efficiency by restricting the angle between the D^* and the lepton.

At this stage, our sample of candidates contains not only $D^*\ell\bar{\nu}$ decays but also $\bar{B} \to D^{**}\ell\bar{\nu}$ and nonresonant $\bar{B} \to D^*\pi\ell\bar{\nu}$ decays (collectively referred to here as $\bar{B} \to D^*X\ell\bar{\nu}$ decays) and various backgrounds. In order to disentangle the $D^*\ell\bar{\nu}$ from the $D^*X\ell\bar{\nu}$ decays, we use a binned maximum likelihood fit [8] to the $\cos\theta_{B-D^*\ell}$ distribution. In this fit, the normalizations of the various background distributions are fixed, and those for $D^*\ell\bar{\nu}$ and $D^*X\ell\bar{\nu}$ float.

The distributions of the $D^*\ell\bar{\nu}$ and $D^*X\ell\bar{\nu}$ decays are taken from Monte Carlo simulation [9]. We generate $D^*\ell\bar{\nu}$ decays according to the form factors of Ref. [10] and reweight the events to reflect the form-factor parameters found in this analysis. Radiative $B \to D^*\ell\bar{\nu}\gamma$ decays, modeled by PHOTOS [11], are treated as signal. Nonresonant $\bar{B} \to D^*\pi\ell\bar{\nu}$ decays are modeled using the results of [12], and $\bar{B} \to D^{**}\ell\bar{\nu}$ decays are modeled using the ISGW2 form factors [13].

We account for five classes of background: continuum, combinatoric, uncorrelated, correlated, and fake leptons. (i) Continuum background from $e^+e^- \to q\bar{q}$, which amounts to about 3.5% of the candidates in the region $-1 \leq \cos\theta_{B-D^*\ell} \leq 1$ (the "signal region"), is measured using offresonance data taken below the $B\bar{B}$ threshold. We normalize the $\cos\theta_{B-D^*\ell}$ distribution to the ratio of on- to off-resonance luminosities, correcting for the small energy dependence of the continuum cross section. (ii) Combinatoric background events, those in which one or more of the particles in the D^* candidate does not come from a true D^* decay, contribute 8% (38%) of the

candidates in the D^{*+} (D^{*0}) signal region. We take the $\cos\theta_{B-D^*\ell}$ distribution of combinatoric background events from a Δm sideband, (155, 165) MeV/c^2 for D^{*+} and (147, 165) MeV/c^2 for D^{*0}, and normalize using a fit to the Δm distribution in each w bin. (iii) Uncorrelated background, which accounts for approximately 5% of the candidates in the signal region, arises when the D^* and lepton come from the decays of different B mesons. Most of this background consists of a D^* meson combined with a secondary lepton (i.e., from $b \to c \to s\bar{\ell}\nu$) because primary leptons from the other B have the wrong charge correlation in the absence of $B^0 - \bar{B}^0$ mixing or $\bar{D}^*$ production from the hadronization of the $\bar{c}$ in $b \to c\bar{c}s$. We obtain the uncorrelated $\cos\theta_{B-D^*\ell}$ distribution from Monte Carlo simulation, normalizing to the inclusive D^* production rate observed in our data (in two D^* momentum bins), the measured primary and secondary lepton decay rates [14], the estimated decay rate for modes in the $\bar{B} \to D^*\bar{D}^{(*)}\bar{K}^{(*)}$ family [15,16], and the measured $B^0 - \bar{B}^0$ mixing rate [16]. (iv) Correlated background events are those in which the D^* and lepton are daughters of the same B, but the decay was not $\bar{B} \to D^*\ell\bar{\nu}$ or $\bar{B} \to D^*X\ell\bar{\nu}$. The most common sources are $\bar{B} \to D^*\tau^-\bar{\nu}$ followed by leptonic τ decay and $\bar{B} \to D^*D_s^-$ followed by semileptonic decay of the D_s^-. This background accounts for fewer than 0.5% of the candidates in the signal region and is estimated using Monte Carlo simulation. (v) Finally, hadrons misidentified as leptons contribute fewer than 0.5% of candidates in the signal region.

Having obtained the distributions in $\cos\theta_{B-D^*\ell}$ of the signal and background components, we fit for the yields of $D^*\ell\bar{\nu}$ and $D^*X\ell\bar{\nu}$ decays in each w bin. Representative fits are shown in Fig. 1. The quality of the fits is good, as is agreement between the data and fit distributions outside the fitting region. The fit results also accurately predict the D^* energy distribution and the lepton momentum spectrum of the data.

Given the measured $D^*\ell\bar{\nu}$ yields in ten bins of w, we fit for the partial rate [17]

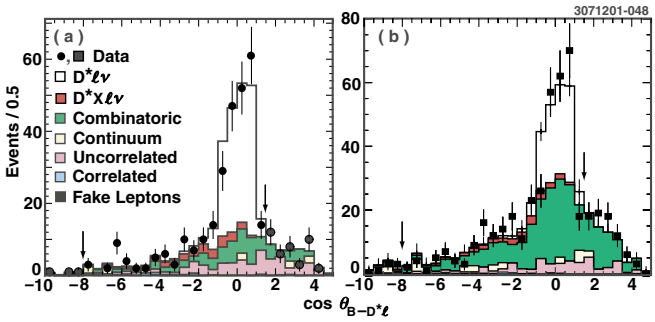

FIG. 1 (color online). The candidate yields for the $1.10 < w < 1.15$ bin with the results of the fit superimposed for (a) $D^{*+}\ell\bar{\nu}$ and for (b) $D^{*0}\ell\bar{\nu}$. The fit uses the region between the arrows.

$$\frac{d\Gamma}{dw} = \frac{G_F^2}{48\pi^3}\mathcal{K}(w)|V_{cb}|^2\mathcal{F}^2(w), \tag{2}$$

where $\mathcal{K}(w)$ is a known function of kinematic variables and $\mathcal{F}(w)$ is the form factor. For our fit we use a form-factor parametrization [10] informed by HQET and dispersion relation constraints [18]. We take the form-factor ratios $R_1(1)$ and $R_2(1)$ from a previous measurement [19] that agrees with theoretical expectations [20]. The slope ρ^2 of the form factor at $w = 1$ is the only shape parameter; it varies in our fit.

We fit our $D^*\ell\bar{\nu}$ yields as a function of w for $|V_{cb}|\mathcal{F}(1)$ and ρ^2. We minimize the sum of χ^2 for $D^{*+}\ell\bar{\nu}$ and $D^{*0}\ell\bar{\nu}$, each of which compares the measured and expected yields in the ten reconstructed w bins. For each mode,

$$\chi^2 \equiv \sum_{i=1}^{10} \frac{[N_i^{\rm obs} - \sum_{j=1}^{10}\epsilon_{ij}N_j]^2}{\sigma^2_{N_i^{\rm obs}}}, \tag{3}$$

where $N_i^{\rm obs}$ is the yield in the ith w bin, N_j is the number of decays in the jth w bin, and the matrix ϵ_{ij} accounts for the reconstruction efficiency and the smearing in w. The smearing is of order half the bin size, so the matrix ϵ is nearly diagonal, with diagonal entries $\approx$0.04–0.13. In the above,

$$N_j \equiv 4f N_{\Upsilon(4S)}\mathcal{B}_{D^*}\mathcal{B}_{D^0}\tau_B\int_{w_j} dw\,\frac{d\Gamma}{dw}, \tag{4}$$

where τ_B is the B^- or $\bar{B}^0$ lifetime [16], $\mathcal{B}_{D^*}$ is the $D^* \to D^0\pi$ branching fraction [16], $\mathcal{B}_{D^0}$ is the $D^0 \to K^-\pi^+$ branching fraction [21], $N_{\Upsilon(4S)}$ is the number of $\Upsilon(4S)$ events in the sample, and f represents f_{00} (f_{+-}), the $\Upsilon(4S) \to B^0\bar{B}^0$ (B^+B^-) branching fraction. We use the result of [22] for $(f_{+-}/f_{00})\,(\tau_+/\tau_0)$ as a constraint in the fit, assuming $f_{00} + f_{+-} = 1$. We assume that $B^- \to D^{*0}\ell\bar{\nu}$ and $\bar{B}^0 \to D^{*+}\ell\bar{\nu}$ have identical partial widths and form factors. We fit for three parameters: $|V_{cb}|\mathcal{F}(1)$, ρ^2, and f_{+-}.

The result of the fit is shown in Fig. 2. We find $|V_{cb}|\mathcal{F}(1) = 0.0431 \pm 0.0013 \pm 0.0018$, $\rho^2 = 1.61 \pm 0.09 \pm 0.21$, and $f_{+-} = 0.521 \pm 0.012$, where the errors are statistical and systematic. The fit χ^2 is 16.8/18 d.o.f., and the correlation coefficient between $|V_{cb}|\mathcal{F}(1)$ and ρ^2 is 0.86, which becomes 0.22 after including systematic correlations. Integrated over w, these parameters give $\Gamma = 0.0394 \pm 0.0012 \pm 0.0026\ {\rm ps}^{-1}$, implying the branching fractions $\mathcal{B}(\bar{B}^0 \to D^{*+}\ell\bar{\nu}) = (6.09 \pm 0.19 \pm 0.40)\%$ and $\mathcal{B}(B^- \to D^{*0}\ell\bar{\nu}) = (6.50 \pm 0.20 \pm 0.43)\%$. Separate $D^{*+}\ell\bar{\nu}$ and $D^{*0}\ell\bar{\nu}$ fits give consistent results. For determination of $|V_{cb}|\mathcal{F}(1)$, the charged (neutral) D^* decay mode has a weight of 0.68 (0.32).

These results are larger than the previous CLEO measurement [23], which was based on approximately half of the data used in the present analysis. When we reanalyze that subset of the data using the new analysis, but the same form factor that was used previously, we find consistent

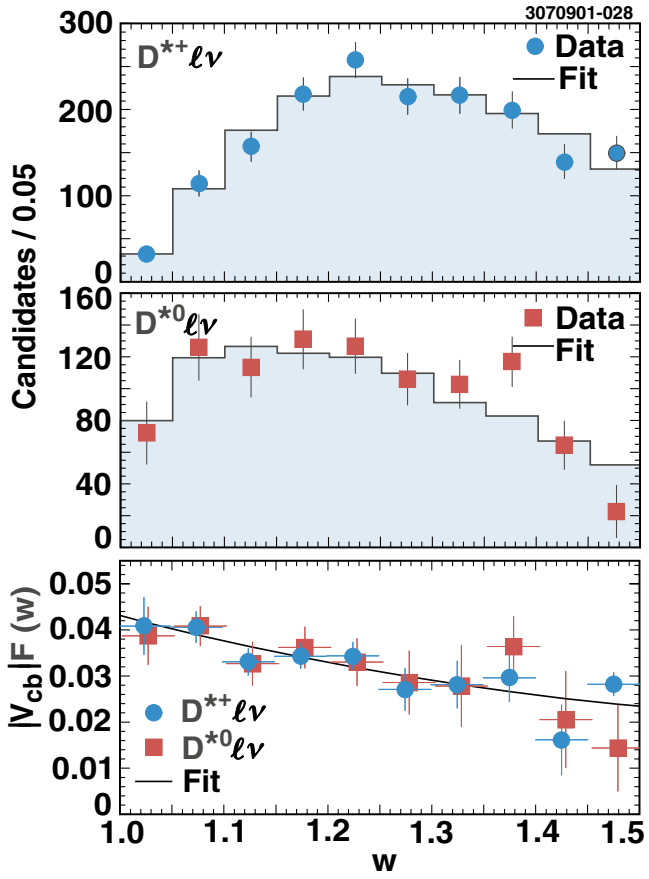

FIG. 2 (color online). The results of the fit to the w distribution. The top figure shows the $D^{*+}\ell\bar{\nu}$ yields (solid circles) with the results of the fit superimposed (histogram). The middle figure shows the same for $D^{*0}\ell\bar{\nu}$. The bottom figure displays $|V_{cb}|\mathcal{F}(w)$, where the solid circles (squares) are derived from the $D^{*+}\ell\bar{\nu}$ ($D^{*0}\ell\bar{\nu}$) yields after correcting for efficiency, smearing, and all terms in the differential decay rate apart from $|V_{cb}|\mathcal{F}(w)$. The curve shows the result of the fit.

results within the systematic errors that are different between the two analyses. The use of the new form factor accounts for a 6% increase in $|V_{cb}|\mathcal{F}(1)$, and accounting for final-state radiation gives an increase of 2.4%. Beyond these technical improvements in the new analysis, it includes twice the luminosity and has higher efficiency, giving increased statistical precision. The results in this Letter supersede those reported in Ref. [23].

The systematic uncertainties are summarized in Table I. The dominant systematic uncertainties arise from our background estimations and from our knowledge of the slow-pion reconstruction efficiency.

We test that the combinatoric candidates in the Δm sideband have the same $\cos\theta_{B-D^*\ell}$ distribution as the background events in the peak region by applying our procedure to Monte Carlo simulated events. The systematic uncertainty is the difference between the results obtained using the true Monte Carlo background and those obtained using the sideband subtraction. We also vary the function used to normalize the Δm sideband. The main source of uncertainty from the uncorrelated background is the branching fraction of the $\bar{B} \to D^* \bar{D}^{(*)} \bar{K}^{(*)}$ decays, which we vary by $\pm 50\%$. Smaller effects arise from the primary and secondary lepton rates and from the uncertainty in $B^0 - \bar{B}^0$ mixing. We assess the uncertainty arising from the correlated background by varying by 50% the branching fractions of the contributing modes.

TABLE I. The fractional systematic uncertainties.

Source	$\lvert V_{cb}\rvert\mathcal{F}(1)$ (%)	ρ^2 (%)	Γ (%)
Continuum background	0.0	0.2	0.1
Combinatoric background	1.6	2.9	1.3
Uncorrelated background	0.7	1.0	0.5
Correlated background	0.1	0.6	0.8
Fake leptons	0.0	0.3	0.2
Slow π finding	2.1	2.8	2.8
Vertex reconstruction	1.5	1.6	2.9
K, π, and ℓ finding	1.0	0.0	1.9
Lepton ID	0.8	0.6	1.1
B momentum and mass	0.1	0.1	0.2
$D^*X\ell\bar{\nu}$ model	0.3	1.6	0.9
Final-state radiation	0.7	0.3	1.1
Number of $B\bar{B}$ events	0.9	0.0	1.8
τ_B and branching fractions	1.8	0.0	3.5
$R_1(1)$ and $R_2(1)$	1.4	12.0	1.8
Total	4.3	13.0	6.6

A major source of uncertainty for the analysis is the reconstruction efficiency of the slow pion from the D^* decay. Because of the small energy release in D^* decay, the slow-pion momentum is correlated with w. Thus, for D^{*+}, the efficiency is small near $w = 1$ for low-momentum pions and increases rapidly over the next few w bins, while the efficiency for $\pi^0 \to \gamma\gamma$ is more uniform in w. We have explored the detection efficiencies as a function of event environment (nearby tracks or showers), drift chamber performance (single measurement resolution and efficiency), vertexing requirements, calorimeter simulation (noise, nonlinearities, and shower simulation threshold), and description of the detector material in our simulation. We vary the amount of noise in the calorimeter simulation and introduce possible residual nonlinearities in the energy scale. These variations are constrained by $m(\gamma\gamma)$ and lateral shower shape distributions from an independent sample of π^0 candidates from our data. The uncertainty in $|V_{cb}|\mathcal{F}(1)$ is dominated by uncertainties in the number of interaction lengths in the inner detector (1.3%) and the vertexing efficiency (1.5%).

We determine the tracking efficiency uncertainties for the lepton and the K and π forming the D^0 in the same study used for the slow pion from the D^{*+} decay. These uncertainties are confirmed in a study of 1-prong versus 3-prong τ decays. The efficiency for identifying electrons (muons) has been evaluated using radiative Bhabha (μ-pair) events embedded in hadronic events, and has an

uncertainty of 2.6% (1.6%). Separate electron and muon analyzes of our data give consistent results.

Our analysis requires knowledge of the $\cos\theta_{B-D^*\ell}$ distribution of the $D^*X\ell\bar{\nu}$ contribution. This distribution in turn depends on both the poorly known branching fractions of contributing modes and their form factors. We note that the $\bar{B} \to D^*\pi\ell\bar{\nu}$ and $\bar{B} \to D_1\ell\bar{\nu}$ modes have the largest and smallest mean $\cos\theta_{B-D^*\ell}$. We therefore repeat the analysis, first using pure $\bar{B} \to D^*\pi\ell\bar{\nu}$ to describe our $D^*X\ell\bar{\nu}$ decays and then using pure $\bar{B} \to D_1\ell\bar{\nu}$ to describe these decays, and we take the larger of the two excursions as our systematic error.

Finally, the form-factor ratios R_1 and R_2 affect the lepton spectrum and therefore the fraction of candidates satisfying our lepton momentum requirements. To assess this effect, we vary R_1 and R_2 within their measurement errors, taking into account their correlation.

Using a recent lattice calculation [24] that yields $\mathcal{F}(1) = 0.919^{+0.030}_{-0.035}$, our result for $|V_{cb}|\mathcal{F}(1)$ implies

$$|V_{cb}| = 0.0469 \pm 0.0014 \pm 0.0020 \pm 0.0018\,. \quad (5)$$

Our result is the most precise to date and is somewhat higher than but marginally consistent with other measurements [25]. However, we note that our ability to reconstruct $\cos\theta_{B-D^*\ell}$ makes our analysis approximately 4 times less sensitive to the poorly known $D^*X\ell\bar{\nu}$ background and allows us to constrain it with the data. This value of $|V_{cb}|$ is also somewhat higher than that obtained from inclusive semileptonic B decays [26]. If confirmed, this discrepancy could signal a violation of quark-hadron duality. A larger value of $|V_{cb}|$ affects constraints on the CKM unitarity triangle, reducing expectations for indirect CP violation in the B system.

We gratefully acknowledge the effort of the CESR staff in providing us with excellent luminosity and running conditions. We thank A. Kronfeld, W. Marciano, and M. Neubert for helpful discussions. This work was supported by the National Science Foundation, the U.S. Department of Energy, the Research Corporation, and the Texas Advanced Research Program.

[1] N. Cabibbo, Phys. Rev. Lett. **10**, 531 (1963); M. Kobayashi and T. Maskawa, Prog. Theor. Phys. **49**, 652 (1973).

[2] L.-L. Chau and W.-Y. Keung, Phys. Rev. Lett. **53**, 1802 (1984); J. D. Bjorken, Phys. Rev. D **39**, 1396 (1989); C. Jarlskog and R. Stora, Phys. Lett. B **208**, 268 (1988); J. L. Rosner, A. I. Sanda, and M. P. Schmidt, in *Proceedings of the Workshop on High Sensitivity Beauty Physics at Fermilab, Batavia, Illinois, 1987*, edited by A. J. Slaughter, N. Lockyer, and M. Schmidt (Fermilab, Batavia, Illinois, 1988), p. 165; C. Hamzaoui, J. L. Rosner, and A. I. Sanda, *ibid.*, p. 215.

[3] See, for example, A. J. Buras, M. E. Lautenbacher, and G. Ostermaier, Phys. Rev. D **50**, 3433 (1994).

[4] The charge conjugate modes are implied.

[5] M. B. Voloshin and M. Shifman, Sov. J. Nucl. Phys. **47**, 511 (1988); N. Isgur and M. Wise, Phys. Lett. B **232**, 113 (1989); **237**, 527 (1990); M. Neubert, *ibid.* **264**, 455 (1991).

[6] Described more fully in CLEO Collaboration, Report No. CLNS 01/1774 (to be published).

[7] Y. Kubota *et al.*, Nucl. Instrum. Methods Phys. Res., Sect. A **320**, 66 (1992).

[8] R. Barlow and C. Beeston, Comput. Phys. Commun. **77**, 219 (1993).

[9] R. Brun *et al.*, GEANT 3.15, CERN Report No. DD/EE/84-1 (1987).

[10] I. Caprini, L. Lellouch, and M. Neubert, Nucl. Phys. **B530**, 153 (1998).

[11] E. Barberio and Z. Wąs, Comput. Phys. Commun. **79**, 291 (1994).

[12] J. L. Goity and W. Roberts, Phys. Rev. D **51**, 3459 (1995).

[13] D. Scora and N. Isgur, Phys. Rev. D **52**, 2783 (1995); N. Isgur *et al.*, Phys. Rev. D **39**, 799 (1989).

[14] B. Barish *et al.*, Phys. Rev. Lett. **76**, 1570 (1996).

[15] CLEO Collaboration, Report No. CONF 97-26, 1997.

[16] D. E. Groom *et al.*, Eur. Phys. J. C **15**, 1 (2000).

[17] J. D. Richman and P. R. Burchat, Rev. Mod. Phys. **67**, 893 (1995).

[18] C. G. Boyd, B. Grinstein, and R. F. Lebed, Phys. Rev. D **56**, 6895 (1997).

[19] J. Duboscq *et al.*, Phys. Rev. Lett. **76**, 3898 (1996).

[20] M. Neubert, Phys. Rep. **245**, 259 (1994).

[21] We use the average of R. Barate *et al.*, Phys. Lett. B **403**, 367 (1997) and M. Artuso *et al.*, Phys. Rev. Lett. **80**, 3193 (1998), which indicate their treatment of final-state radiation.

[22] J. P. Alexander *et al.*, Phys. Rev. Lett. **86**, 2737 (2001).

[23] B. Barish *et al.*, Phys. Rev. D **51**, 1014 (1995).

[24] S. Hashimoto *et al.*, Report No. FERMILAB-PUB-01/317-T; hep-ph/0110253. We apply a QED correction of +0.007.

[25] D. Buskulic *et al.*, Phys. Lett. B **395**, 373 (1997); G. Abbiendi *et al.*, *ibid.* **482**, 15 (2000); P. Abreu *et al.*, *ibid.* **510**, 55 (2001); K. Abe *et al.*, *ibid.* **526**, 258 (2002).

[26] D. Cronin-Hennessy *et al.*, Phys. Rev. Lett. **87**, 251808 (2001).